Journal of Wind Engineering and Industrial Aerodynamics, 49 (1993) 167–176
Elsevier

Cross Flow Response of Slender Circular-Cylindrical Structures: Prediction Models and Recent Experimental Results

H.M. Blackburn and W.H. Melbourne

Department of Mechanical Engineering, Monash University, Clayton 3168, Australia.

Abstract

Wind tunnel tests on a smooth circular cylinder in high Reynolds number smooth and turbulent flows have produced data which may be compared with full scale measurements and with the parameters of cross flow response prediction models. The task of cross flow response prediction is reviewed and the experimental results are discussed in relation to one of a class of negative aerodynamic damping models for response prediction.

1. INTRODUCTION

Prediction of the cross flow vortex induced vibration response of slender structures of circular cross section is one of the 'classical' problems of bluff body aeroelasticity. For a number of reasons, it is difficult to make accurate predictions: details of the flow and the associated forces exerted on the body are poorly understood and are strongly influenced by a number of factors such as Reynolds number, surface roughness, freestream turbulence and structure geometry (e.g., aspect ratio, taper); there are significant aeroelastic effects even at low motion amplitudes, again not well understood; at moderate response amplitudes there is interaction between along and cross flow motion and the probability density of response amplitude changes in form as amplitude increases.

In flows with moderate to high free stream turbulence intensity, typical of civil and offshore engineering applications, cross flow forces are induced both by vortex shedding and by buffeting due to the cross flow components of incident turbulence. As noted above, turbulence also influences vortex shedding, and it is not a simple matter to partition the effect of turbulence into effects on vortex shedding and cross flow buffeting; such a partition depends heavily on the concept of a 'spectral gap' between large-scale (low frequency) turbulent fluctuations and the length scales of vortex shedding.

In this paper, we present results of a wind tunnel investigation (Blackburn 1992) of lift forces on a circular cylinder conducted at high Reynolds numbers ($1 \times 10^5 < Re < 5 \times 10^5$) and free stream turbulence intensities [I_u = (standard deviation on mean velocity) = $\sigma_u/U \leq 18\%$] and discuss them in relation to response prediction models used in wind engineering.

2. WIND TUNNEL MODEL

Measurements of lift forces on narrow segments of a smooth circular cylinder were conducted in an insertable 2 m×1 m working section of the Department's 450 kW boundary layer wind tunnel. Six lift transducers were mounted at $0.75\,D$ (D is cylinder diameter) centres on the 4.5:1 aspect ratio cylinder model (see Fig. 1) and measurements could be obtained simultaneously from all transducers. In addition, the cylinder could be forced to oscillate cross flow at amplitudes $y \leq 3\%\,D$; cancellation of the inertial

component of transducer signals was carried out using on-board accelerometers and an off-line adaptive digital filter technique.

The range of Reynolds numbers which could be obtained was 1×10^5 to 5×10^5 and the oscillation frequency (i.e., reduced velocity $V_r = U/fD$) was independently variable in the range 3–6. Turbulence screens were inserted upstream of the contraction to obtain a range of longitudinal turbulence intensities from 0.6% ('smooth flow') to 18%. The ratio of longitudinal turbulence integral scale L_u^x to cylinder diameter D was approximately 0.5 for the turbulent flow results reported here. Tunnel blockage was 10% and in light of the uncertainty of correction methods in the flow regimes investigated, no correction was applied to the results.

More detailed descriptions of the experimental equipment and techniques may be found in Blackburn and Melbourne (1991), Blackburn (1992).

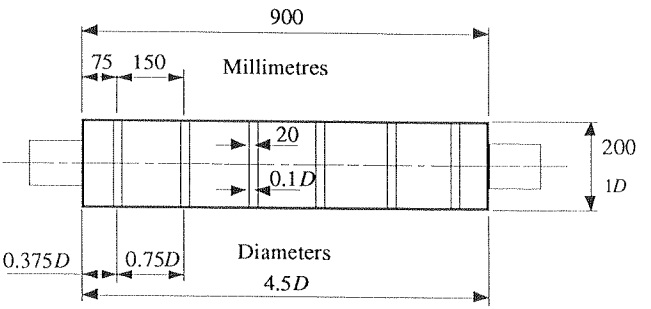

Figure 1. Diagram of cylinder model, showing the layout of the six ($0.1\,D$) lift transducers along the cylinder axis. Air-gaps between the various segments were sealed using thin elastomeric film and the $4.5\,D$ length spanned between large end plates.

3. RESULTS FROM OSCILLATING CYLINDER TESTS

When the cylinder was forced to oscillate sinusoidally perpendicular to the mean flow, motion correlated forces were observed in addition to forces uncorrelated with motion. The motion-correlated forces were partitioned into components correlated with cylinder velocity and acceleration. At most half the total lift variance was correlated with motion when the correlations were obtained over many vortex shedding periods. The most substantial motion-correlated force coefficients were observed in smooth subcritical flow at reduced velocities near critical ($V_r \simeq 5$); the variation of the forces with reduced velocity was similar to that found in previous experiments, as reported by Blackburn and Melbourne (1991). It is thought that form of the variation in force coefficients with reduced velocity and motion amplitude found in smooth subcritical flow is relevant to predictions at higher, transcritical Reynolds numbers in turbulent flows with large L_u^x/D and that the lower values observed in the flows of higher I_u were related to the comparatively low experimental value of L_u^x/D. The results reported in this section are for smooth subcritical flows, with $Re \simeq 1.6 \times 10^5$.

The motion-correlated forces are reported in terms of a coefficient of added mass, C_a and an aerodynamic damping parameter K_a. If l_a and l_v are respectively acceleration- and velocity-correlated lift forces per unit length, and $\ddot{y}$, $\dot{y}$ the acceleration and velocity

of the cylinder in sinusoidal motion, then

$$l_a = -C_a \cdot \rho \frac{\pi D^2}{4} \cdot \ddot{y} \qquad \text{and} \qquad l_v = K_a \cdot 16f \cdot \rho \frac{\pi D^2}{4} \cdot \dot{y} \, .$$

At a fixed amplitude of motion, the highest values of C_a were observed at slightly lower reduced velocities than the highest values of K_a, consistent with a change in the average phase of vortex shedding with respect to the cylinder motion cycle, as described for example in Zdravkovich 1982. During the experiments, three different amplitudes of motion were used, allowing the values of C_a and K_a to be extrapolated to zero motion amplitude limits C_{a0} and K_{a0} as shown in Fig. 2 where this process has been carried out using the peak values of C_a and K_a at each amplitude $\alpha = y_{\max}/D$. As can be observed in the figure, there was a distinct amplitude effect, with the coefficients falling approximately linearly with increasing amplitude; fitted lines gave the following values: $C_{a0} = 27.5$, $K_{a0} = 6.5$, $\partial C_a/\partial\alpha = -430$, $\partial K_a/\partial\alpha = -85$.

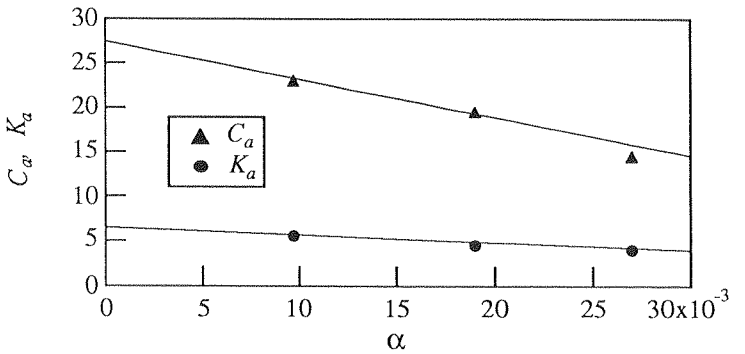

Figure 2. Highest positive values of C_a(▲) and K_a(●) in smooth subcritical flow ($Re = 1.6 \times 10^5$), as functions of dimensionless oscillation amplitude $\alpha = y_{\max}/D$.

4. RESULTS FROM FIXED CYLINDER IN TURBULENT FLOW

In smooth flow, the transition to critical flow began at $Re \simeq 2.2 \times 10^5$; at higher Reynolds numbers, there were no signs of Strouhal peaks in the lift spectra, which dropped monotonically from low frequencies. The absence of high Strouhal number vortex shedding in the supercritical regime, as opposed to shedding with $St = 0.48$ observed in some experiments, (e.g., Schewe 1983), is thought to be a consequence of the moderate cylinder aspect ratio of 4.5:1, in accordance with the results of Achenbach and Heinecke (1981), who found high frequency vortex shedding in the supercritical regime on a 6.75:1 cylinder, but no organized shedding on a 3.75:1 cylinder. In the precritical regime, values of sectional coefficients of lift fell with increasing Reynolds numbers and the Strouhal number remained near 0.20, while the spanwise correlation of lift, as measured by the correlation length, remained relatively constant near $3.75\,D$ right up to the critical transition when it fell suddenly at first, then more gradually with increasing Re to reach a value near $1\,D$ (see Fig. 4).

It was found that the addition of intense freestream turbulence to the flow had a pronounced effect on the lift forces acting on the cylinder over the range of Re. At the

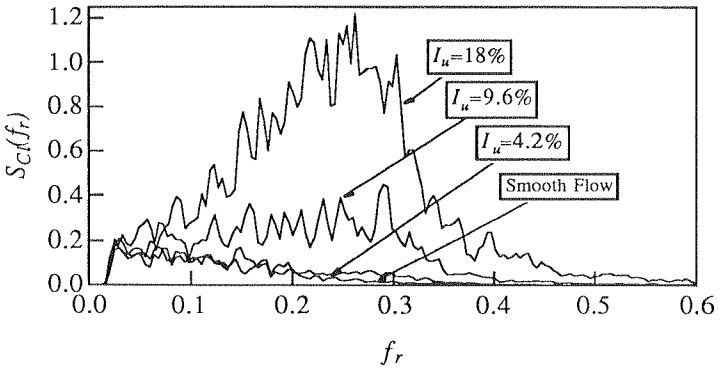

Figure 3. Spectra of lift coefficient measured at $Re \simeq 4.6 \times 10^5$ with the cylinder held fixed, showing the influence of longitudinal turbulence intensity I_u. In all but the smooth flow, $L_u^x/D = 0.5$. Spectra have been normalized such that their areas equal $\sigma_{C_l}^2$. Frequencies are expressed dimensionlessly; $f_r = fD/U$.

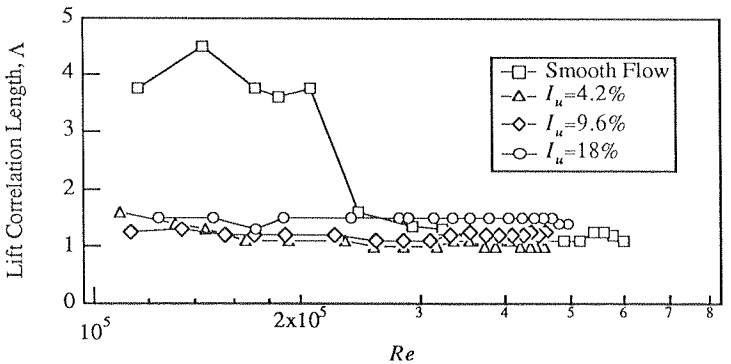

Figure 4. Correlation length of lift force Λ (expressed in terms of cylinder diameters) for fixed cylinder as a function of Re, showing the influence of turbulence intensity.

lowest turbulence intensities ($I_u \simeq 4\%$), the main effect of turbulence was to promote the transition to the supercritical regime at lower Reynolds numbers than in smooth flow; once the transition was complete, there was effectively no difference between the lower turbulence intensity flows and the smooth flow, at least for $Re < 6 \times 10^5$. For $I_u = 9.6\%$, however, values of lift coefficient standard deviation σ_{C_l} were higher than in the supercritical smooth flow, and increased somewhat with Reynolds number to reach peak values of $\sigma_{C_l} \simeq 0.24$ at $Re \simeq 5 \times 10^5$. Lift spectra differed in shape for those for supercritical smooth flow, with the appearance of a broad plateau in lift force spectral density over a range of reduced frequencies, in contrast to the monotonic decline observed for smooth flow, as shown in Fig. 3. Spanwise correlation lengths remained close to values for smooth supercritical flows over the range of Reynolds number. When turbulence intensity was increased again to $I_u = 18\%$, lift coefficients increased further, also exhibiting a slight upward trend with Reynolds number, reaching values of $\sigma_{C_l} \simeq 0.42$ at $Re \simeq 5 \times 10^5$. Spectra of lift force showed evidence of increased organization of

vortex shedding, with the appearance of a definite but very broad Strouhal peak centred near $St = 0.23$. In addition, spanwise correlation lengths of lift forces rose to values near $1.5\,D$, as shown in Fig. 4.

5. DISCUSSION

No single procedure has yet become accepted (i.e., codified) for the prediction of cross flow response of slender cylindrical structures in flows of air, in contrast with the prediction of the along flow response of such structures in turbulent flows, where the 'Gust Factor' method is now commonly used. In this section we briefly review some of the available prediction models, concentrating on those which are oriented more towards civil engineering applications, where predicted response amplitudes must typically be limited to less than $5\%\,D$ to avoid the possibility of unstable lock-in behaviour.

The greatest amplitude of vortex induced response occurs when vortex shedding and structural natural frequencies coincide and the prediction models concentrate on this condition. It is important to note however that the largest cross flow response amplitudes for a particular structure may be induced by cross flow buffeting by turbulence, since the buffeting forces grow approximately with the square of the flow speed while the peak vortex induced responses may occur at flow speeds near the lower end of the design envelope. For structures under examination for vortex induced vibrations in air, response occurs mainly at the natural frequencies of the structure even if the vortex shedding forces have a significant bandwidth. This is not necessarily true when the mass-damping parameter $K_s = \zeta_s m/\rho D^2$ is *very* low, e.g., in flows of water (ζ_s is fraction of critical structural damping, m is structural mass per unit length and ρ is fluid density; the Scruton parameter $2\delta m/\rho D^2 = 4\pi K_s$.).

A number of different models for predicting structural response of slender cylindrical structures to vortex shedding have been advanced; the models tend to fall naturally into two main groups; those used to predict low and high amplitude motions. In the regime where high [$\mathcal{O}(D)$] amplitudes of response are observed (K_s is small) there have been two major sets of models, the *wake oscillator* and *correlation length* types, as discussed for example by Blevins (1977). For the low amplitude ($\sigma_\alpha \leq 2\%\,D$) regime the models tend to be of the *forced random vibration* type, since the responses show narrow-band random characteristics and the observed variation in response amplitudes with changes in ζ_s matches that expected for forced random vibrations of lightly-damped structures. *Negative (aerodynamic) damping* models provide a transition between the low and high amplitude response regimes. We will concentrate on the forced random vibration and negative damping models as being most suitable for the majority of structures where response amplitudes must be limited to low levels.

5.1. Forced Random Vibration and Negative Damping Models for Cross-Flow Response Prediction

As mentioned above, the most rational models for estimation of comparatively low response amplitudes ($\sigma_\alpha \leq 2\%$) are based in random vibration theory as applied to line-like structures. If, as is typically the case for the lowest vibration modes of lightly-damped slender structures, there is no significant frequency overlap between the responses of the different modes, the theory requires a description of the spatial distribution along the structure of the co-spectra (real parts of the cross-spectra) of vortex shedding loads. The first significant model of this type for civil engineering applications was that of Vickery and Clark (1972); the 'broad band' procedure of ESDU 85038 is very similar in character. It is assumed that the bandwidth of the excitation is much

larger than that of the resonant peak of the admittance function; the inaccuracies incurred by the assumption are likely to be small compared to the uncertainties in the model parameters.

The general form of the response standard deviation predicted by these methods is

$$\sigma_\alpha = \frac{1}{D_{\text{ref}}} \cdot \sqrt{\frac{\pi f_j S(f_j)}{4\mathcal{K}_j}} \Big/ \sqrt{\zeta_{s_j}} \,.$$

Here, f_j is the frequency of oscillation of the jth vibration mode, $\mathcal{K}_j$ is the modal stiffness for that mode, and $S(f_j)$ is the value of the spectral density of the mode-generalized cross flow force at the frequency f_j. D_{ref} is some reference diameter, and σ_α is the standard deviation modal response amplitude made dimensionless with respect to D_{ref}. $S(f_j)$ is obtained as an integral of the product of the co-spectral density of cross flow force and the vibration mode shape of the jth vibration mode, and contains all the aerodynamic information in the model. Typically a number of simplifying assumptions are used express the co-spectral density of lift in terms of the local (sectional) lift autospectra and the correlation between lift forces at different spanwise locations.

Negative damping models account for experimentally-observed motion-correlated lift forces (as described in § 3) by introducing forces proportional to structural motion to the modelling equations. Acceleration-correlated forces (expressed by C_a) are typically ignored, since, for structures in air flows at least, they are small in relation to structural stiffness and inertia forces, and would only act to change the structural natural frequencies by a small amount. The velocity-correlated forces are more significant since they may be large in comparison to structural damping forces, while at appropriate reduced velocities they can act in phase with structural motion to reduce the overall system damping; hence the term 'negative damping'. Some form of amplitude-dependence of velocity-correlated forces is often modelled in order to match the experimental observations in tests of freely vibrating cylinders that the amplitude of oscillation reaches some limit as structural damping approaches zero. The most well-developed model of this kind is that described first by Vickery (1978) and subsequently extended by Vickery and Basu (1983, see also Simiu & Scanlan 1986).

5.1.1. Vickery and Basu's model

The model adapts Vickery and Clark's prediction scheme by modifying the overall system damping to account for velocity-correlated forces. The basic assumption used is that the vortex shedding forces and their interaction with cylinder motion may be expressed as the sum of two independent processes, the first being the narrow-band-Gaussian vortex shedding process appropriate for the motionless cylinder, the second modelling velocity-correlated forces as negative aerodynamic damping, the magnitude of which decreases as response amplitude increases. The modelling of the Gaussian vortex shedding forces follows Vickery and Clark, while as described in § 3, the velocity-correlated forces are modelled in terms of an aerodynamic damping parameter K_a. The form adopted for the variation of K_a with α is quadratic:

$$K_a = K_{a0}\left[1 - \left(\frac{\alpha}{\alpha_L}\right)^2\right], \quad \text{or equivalently} \quad \zeta_{\text{aero}} = -\frac{\rho D^2}{m} K_{a0}\left[1 - \left(\frac{\alpha}{\alpha_L}\right)^2\right],$$

the latter for a uniform cylinder oscillating with a uniform mode shape. Here, K_{a0} is the aerodynamic damping parameter in the limit $\alpha \to 0$; α_L is a limiting amplitude,

reached as $K_s \to 0$. This two-parameter model for the velocity-correlated cross flow forces can alternatively be considered in the form of a coefficient of lift forces correlated with structural velocity, i.e.,

$$C_{lv} = \frac{16\pi^2 K_{a0}}{V_r^2}\left[\frac{\alpha - \alpha^3}{\alpha_L^2}\right],$$

showing that K_{a0} can also be considered as a measure of $\partial C_{lv}/\partial\alpha$ at $\alpha = 0$.

The negative aerodynamic damping is incorporated into the random vibration prediction procedure described above by adding it to the structural damping; in the case of a constant-diameter cylinder oscillating with a uniform mode shape in a uniform flow

$$\sigma_\alpha = \frac{1}{D_{\text{ref}}} \cdot \sqrt{\frac{\pi f_j S(f_j)}{4K_j}} \Bigg/ \sqrt{\zeta_s - \frac{\rho D^2}{m} K_{a0}\left[1 - \left(\frac{\sigma_\alpha}{\alpha_L}\right)^2\right]}.$$

Since the vibration is random, it is assumed that the negative aerodynamic damping is a function of the standard deviation amplitude σ_α; likewise the value of α_L is now interpreted as a limiting standard deviation amplitude. Some slight complications in the coefficients are introduced when the assumptions of uniform mode shape, uniform diameter and flow are relaxed, but the form of the equation does not change. The model suggests that large amplitudes of response only arise when K_s drops to reach K_{a0}, and if it falls below this, the amplitude settles at such a level that the overall system damping is zero.

In § 3, it was noted that the experimental dependence of K_a on α was approximately linear in the limit $\alpha \to 0$, with a large value of $\partial K_a/\partial\alpha$, in disagreement with Vickery and Basu's model for the dependence (which has $\partial K_a/\partial\alpha = 0$ as $\alpha \to 0$). The effect of incorporating a linear variation of K_a with α is shown in Fig. 5, where a linear variation is compared with Vickery and Basu's quadratic dependence for the same values of K_{a0} and α_L. It can be seen that the assumed form of variation of K_a with amplitude only has significant effect at values of $K_s < K_{a0}$. In the range of $K_s \gg K_{a0}$, which constitutes the design regime for most civil engineering applications due to fatigue-related constraint on allowable oscillation amplitudes, it is only the value of K_{a0} which is important.

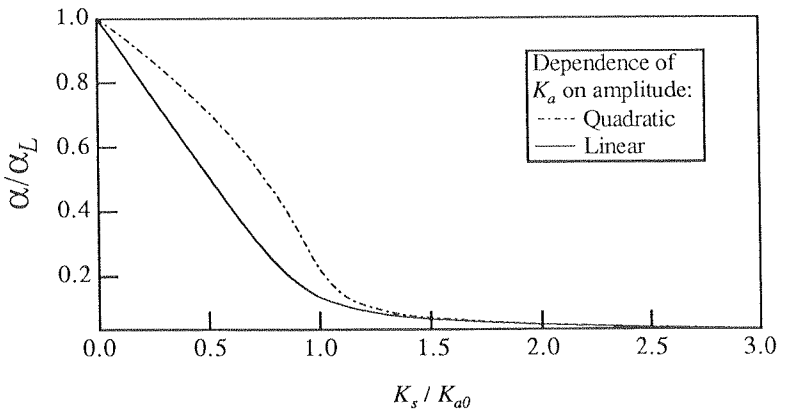

Figure 5. The dependence of response amplitude σ_α on structural damping expressed by $K_s = \zeta_s m/\rho D^2$ for two different forms of the variation of negative aerodynamic damping parameter K_a with amplitude.

5.2. Influence of Free-Stream Turbulence on Lift Forces

If it is possible to separate the effect on cross flow forces of large scales of turbulence from that of the fine scales then the cross flow response due to (large-scale) lateral buffeting may be calculated on a quasi-steady basis. Assuming the aerodynamic admittance to buffeting by large scales of turbulence to be unity over the energy-containing scales, the standard deviation of fluctuating lift force per unit length can be calculated as

$$\sigma_l = \frac{1}{2}\rho U^2 I_v C_d D$$

(where $I_v = \sigma_v/U$ and C_d is the coefficient of drag) so that estimates of the cross flow response of the structure may be made if the characteristics of the turbulence are known.

The separation of large and fine scale effects could be made on the basis of L_u^x/D, although this is made difficult by the slow decay of turbulence energy with frequency, as shown in Fig. 6, where a representative lift force spectrum with a bandwidth appropriate to smooth flow is shown compared to a number of (von Kármán) turbulence spectra of different L_u^x/D but same energy. It might be possible, for example, to regard the turbulence as having a quasi-steady effect for L_u^x/Ds greater than 10, while this would probably be unreasonable for L_u^x/Ds order unity and below. Many full scale flows of engineering interest have L_u^x/D less than 10, but unfortunately it is difficult to achieve length scale ratios greater than unity in most wind tunnels if cylinder diameters are high enough to provide large Reynolds numbers. In addition, turbulence of all scales has significant influence on flow transition phenomena at most Reynolds numbers for flows around circular cylinders, making it difficult to distinguish intensity effects from length scale effects when attempting to establish the aerodynamic admittance to cross-flow buffeting. It may be possible to overcome this problem by conducting tests at lower Reynolds numbers on sections with fixed separation points, giving lower sensitivity to transition phenomena.

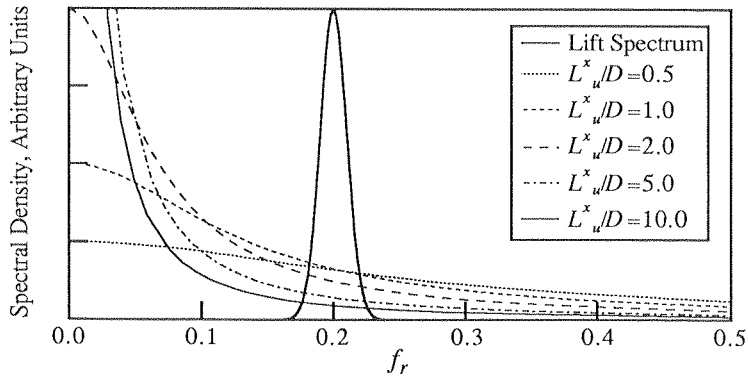

Figure 6. Spectra of turbulence and lift due to vortex shedding, plotted on a common frequency axis, showing the effect of L_u^x/D on relative frequency content. Vertical units of measure are arbitrary, but turbulence spectra are normalized to the same energy.

In the present series of tests, $L_u^x/D \simeq 0.5$, so the influence of turbulence on cross flow force could not be considered quasi-steady. Figure 3 shows the pronounced effect

of variation of turbulence intensity at a fixed L_u^x/D and Reynolds number: increasing intensity produced increased forces and a greater organization of vortex shedding on the evidence of the change in spectral shapes. The influence of turbulence on fluctuating forces is often parametrized by a generalized Taylor number of the form $I_u(L_u^x/D)^n$ where n is negative. Bearman and Morel (1983) argued that while such a parameter has (at least, at present) no theoretical basis for use in separated flows, it may achieve a correlating effect in collapsing experimental results due to fact that it emphasizes the influence of the finer scales of turbulence. Vickery and Daly (1984) presented an analysis of measurements of cross flow forces obtained in full scale tests with Reynolds numbers in the range 1×10^7 to 4×10^7 in which σ_{C_l} was plotted against $I_u(L_u^x/D)^{-1/3}$. Their data are replotted here in Fig. 7, together with values at $Re \simeq 5 \times 10^5$ for the two highest turbulence intensities employed ($I_u = 9.6\%$ and $I_u = 18\%$) in the current tests; it can be seen that those two points follow the trend established by the full scale results.

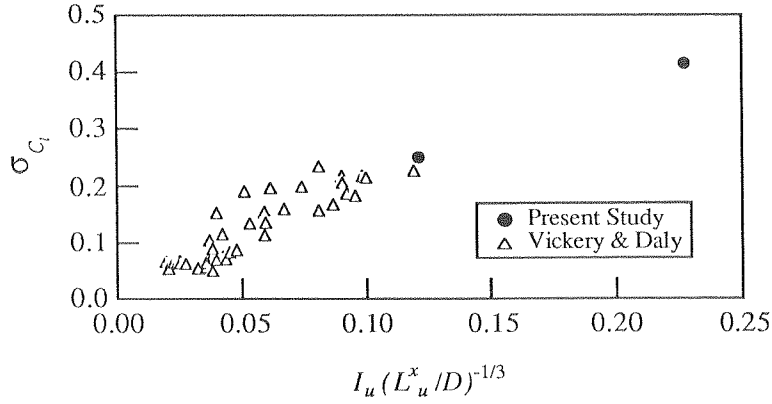

Figure 7. Estimates of turbulence parameters $I_u(L_u^x/D)^{-1/3}$ and sectional coefficients of lift made from full scale results by Vickery and Daly (1984), together with values obtained at the upper end of the Reynolds range ($Re \simeq 5 \times 10^5$) in the present experiments.

5.3. Variation of Correlation Lengths with Reynolds Number

The data of figure 4 represent some of the first measurements of spanwise correlation of lift made in turbulent transcritical flow past a circular cylinder. The increase in spanwise correlation lengths from the $I_u = 9.6\%$ flow to the $I_u = 18\%$ flow supports the evidence of a return to organized vortex shedding provided by the change in spectral shapes in figure 3.

It has been assumed that the values of spanwise correlation length in transcritical flows would be smaller than those in subcritical flows; for example, in Vickery and Basu's model a value of one cylinder diameter is assumed. The value found here, of approximately 1.5 cylinder diameters in a very highly turbulent flow with small L_u^x/D, suggests that in full scale transcritical turbulent flows, where turbulence intensity is similar but L_u^x/D is greater (hence, fluctuations at the scale of the cylinder diameter will be less energetic), the correlation length may be larger still, perhaps approaching values for subcritical flows (3–4 cylinder diameters).

6. CONCLUSIONS

Measurements of the variation of motion correlated forces with oscillation amplitude in smooth subcritical flow showed that the variation of aerodynamic damping parameter K_a with oscillation amplitude α was approximately linear and negative at small amplitudes. This disagrees with the quadratic variation of K_a with α used by Vickery and Basu's response model but is in agreement with the earlier variant of the model, proposed by Vickery in 1978. The difference in form is not significant for the prediction of response in many applications, since designers must usually ensure that the structural mass-damping K_s exceeds K_{a0} in which case it is only the value of K_{a0} which is important in the model, rather than the assumed variation of K_a with α.

The addition of progressively higher intensity freestream turbulence to the flow at first disrupted and then re-established vortex shedding over the Reynolds number range 1×10^5 to 5×10^5. The dependence of σ_{C_l} on $I_u(L_u^x/D)^{-1/3}$ was shown to follow a trend observed in full scale results obtained at higher Reynolds numbers. Re-established vortex shedding was accompanied by an increase in the spanwise correlation of cross flow force to 1.5 cylinder diameters. These effects suggest that future developments of response models could incorporate a variation of σ_{C_l} with $I_u(L_u^x/D)^{-1/3}$ and increase model values of lift correlation lengths in transcritical flows.

7. REFERENCES

Achenbach, E. & Heinecke, E. 1981, On vortex shedding from smooth and rough cylinders in the range of Reynolds numbers from 6×10^3 to 5×10^6, *J Fluid Mech*, **109**, pp. 230–251.

Bearman, P.W. & Morel, T. 1983, Effect of free stream turbulence on the flow around bluff bodies, *Prog Aero Sci*, **20**, pp. 97–123.

Blackburn, H.M. 1992, Lift on an oscillating cylinder in smooth and turbulent flows, PhD thesis, Monash University.

Blackburn, H.M. & Melbourne, W.H. 1991, Lift on an oscillating cylinder in smooth and turbulent flow, in *Proc 8th Int Conf Wind Eng*, London, Ontario, paper 17-2.

Blevins, R.D. 1977, *Flow Induced Structural Vibration*, Van Nostrand Reinhold.

Engineering Sciences Data Unit (ESDU) 1985, *Item 85038. Circular-Cylindrical Structures: Dynamic Response to Vortex Shedding. Pt. 1*, ESDU, London.

Schewe, G. 1983, On the force fluctuations acting on a circular cylinder in crossflow from subcritical up to transcritical Reynolds numbers, *J Fluid Mech*, **133**, pp. 265–285.

Simiu, E. & Scanlan, R.H. 1986, *Wind Effects on Structures*, 2nd edn, Wiley.

Vickery, B.J. 1978, A model for the prediction of the response of chimneys to vortex shedding, in *Proc 3rd Int Symp Design Ind Chimneys*, Munich, pp. 157–162.

Vickery B.J. & Basu, R.I. 1983, Across-wind vibration of structures of circular cross section. Parts 1 & 2, *J Wind Eng Ind Aero*, **12**, pp. 49–97.

Vickery, B.J. & Clark, A.W. 1972, Lift or across-wind response of tapered stacks, *ASCE J Struct Div, ST1*, **98**, pp. 1–20.

Vickery, B.J. & Daly, A. 1984, Wind tunnel modelling as a means of predicting the response of chimneys to vortex shedding, *Eng Struct*, **6**, pp. 364–368.

Zdravkovich, M.M. 1982, Modification of vortex shedding in the synchronization range, *ASME J Fluid Eng*, **104**, pp. 513–517.